

Determination of mangrove forest performance in reducing tsunami run-up using physical models

H. Ismail · A. K. Abd Wahab · N. E. Alias

Received: 8 April 2011 / Accepted: 12 April 2012 / Published online: 4 May 2012
© Springer Science+Business Media B.V. 2012

Abstract Coastal ecosystems such as mangroves fringing tropical coastlines have been recognized as natural protectors of the coastal areas against destructive attack of a tsunami. In this paper, the authors aim to investigate the interaction of a tsunami wave on a typical mangrove forest and to determine its performance in reducing the run-up. A laboratory experiment using a hydraulic flume with a mangrove forest model was carried out in which tests were conducted by varying the vegetation widths of 0, 1, 2 and 3 m and average densities of 8, 6 and 4 trees per 100 cm² using a scale ratio of 1:100. Two conditions of water levels were considered in the experiments at several tsunami wave heights between 2.4 and 14 cm. The dam break method used in the experiments produced two types of waves. At low water condition, a bore was developed and subsequently, a solitary wave was produced during high water. The results of the experiments showed that in general, vegetation widths and densities demonstrate a dampening effect on tsunami run-up. A larger vegetation width was found to be more effective in dissipating the wave energy. The first 1 m width of mangrove forest could reduce 23–32 % during high water and 31–36 % during low water. Increasing the mangrove forest width to 2 and 3 m could further increase the average percentage of run-up reduction by 39–50 % during high water and 34–41 % during low water condition. It was also observed that densities of the mangrove forest do not influence the run-up reduction as significantly as the forest widths. For mangrove forest densities to be significantly enough to reduce more tsunami run-up, an additional density of 4 trees/100 m² needs to be provided. The experiments also showed that mangrove roots are more effective in reducing the run-up compared to the trunks and canopies. The experiments managed to compare and present the usefulness of mangrove forests in dissipating wave energy and results produced are beneficial for initiating design guidelines in determining setback limits or buffer zones for development projects in mangrove areas.

H. Ismail (✉) · A. K. Abd Wahab
Coastal and Offshore Engineering Institute, Universiti Teknologi Malaysia International Campus, Jalan Semarak, 54100 Kuala Lumpur, Malaysia
e-mail: hadibah@ic.utm.my

N. E. Alias
Faculty of Civil Engineering, Universiti Teknologi Malaysia, 81310 Skudai, Johor Bahru, Malaysia

Keywords Tsunamis · Mangroves · Vegetation cover · Run-up · Physical models · Dam break

1 Introduction

Marine ecosystems, such as coastal forests and mangroves fringing tropical coastlines, are very important not only from ecological view points but also from aspects of economical, socio-cultural as well as their physical services to the marine environment. Mangroves also form the physical boundaries for the land-sea interaction, that is at the transition zone between terrestrial and aquatic environments and between coastal areas and the open sea (Moberg and Ronnback 2003).

Since December 26, 2004, the Indian Ocean Tsunami has put a new perspective and high profile on natural disasters such as earthquakes, floods and hurricanes. The United Nations Environment Programme (UNEP)'s Post-Tsunami Assessment Report (February 2005) highlighted that the nearshore impacts of a tsunami are greatly influenced by the vegetation cover of the coastal areas. Expert reports and field observations after this catastrophic event singled out those coastal areas with intact mangroves were found to be less badly affected compared to those whose ecosystems have been damaged or replaced by physical development projects. In some areas of Indonesia, Thailand and Malaysia, mangrove forests saved lives and properties by acting like a giant dampener (Fogarty 2005). The relatively low death toll on the Indonesian island of Simeuleu, close to the earthquake's epicenter, has been attributed partly to the surrounding mangrove forests. These marine ecosystems acted as a natural barrier against strong wave attack. It is thus important to note that the nearshore impacts of the tsunami are greatly influenced not only by the wave energy, but mainly also by the differences in the natural cover or topography of the coastal areas. However, during the March 11, 2011 Great East Japan Tsunami, it was discovered that the pine tree forests in Rikuzentakata unfortunately could not prevent or reduce the tsunami energy. This means that there is a limit of the performance of coastal vegetation against tsunami of this size. It is worth noting, however that mangrove forests are entirely dissimilar to pine trees, in terms of their physical characteristics and anatomy. Hence, the failure of pine trees in Rikuzentakata to prevent or reduce the tsunami size as experienced during the 2011 Great East Japan Tsunami cannot be used to weigh against mangrove forests.

Researchers such as Hiraishi (2000), Kathiresan and Rajendran (2005), Mascarenhas and Jayakumar (2008) and Onrizal et al. (2009) conducted site surveys on the tsunami impact against coastal vegetation just after the 2004 tsunami. All of the findings were presented in the form of qualitative data since the method to calculate the exact impacts was complicated. Presently, substantial analyses of the impact from the 2004 tsunami were able to be conducted using advance technique such as using satellite imageries and numerical modeling. Yanagisawa et al. (2009) used these techniques into their site survey analysis and produced analytical results. They showed that with a 400 m forest width, 26 % of the inundation depth was reduced while a 1,000 m of forest width would reduce about 45 % of the inundation depth at a maximum current velocity of 5 m/s and tsunami heights between 4 and 8 m. However, the model was limited to a 0.15 m stem diameter and 0.2 trees/m² vegetation densities.

In addition to site surveys and numerical modeling, physical models in controlled laboratory conditions were also available although not that many compared to numerical models. These include studies conducted by Harada and Imamura (2002), Hiraishi and

Harada (2003), Harada and Kawata (2005) and Irtem et al. (2009). Hiraishi and Harada (2003) inferred that a mangrove forest with a density of 0.3 trees/m² and a 100 m width could dissipate 50 % of the tsunami wave height. In another study, Irtem et al. (2009) produced results of the run-up reduction on dense pine trees. They discovered that 45 % of the run-up could be reduced. The role of mangrove forest especially in terms of the hydrodynamic aspects was also discussed in detail by Mazda et al. (2007).

In this paper, a physical model to test the performance of different mangrove forest properties in reducing tsunami run-up will be presented. The tests included several experimental runs involving various vegetation widths and densities against several tsunami wave heights at two different water-level conditions.

2 A review of literature

2.1 Tsunami waves

According to Yeh (1991) and Chanson (2005), tsunamis reach the shoreline either by a very slow rise in water level or by a surging bore. In the former situation, no wave breaking takes place, and the horizontal run-up is a slow and gradual flooding of the land. In the latter case, wave breaking may occur before the tsunami reaches the coastline and the wave front becomes a turbulent surge. After wave breaking in shallow waters, the tsunami waves may surge on dry or inundated coastal plains, in a manner somewhat similar to a dam break wave. Such tsunami surges were witnessed in Western Aceh, Banda Aceh, Indonesia and Khao Lak, Patong, Thailand on December 26, 2004 (Chanson 2005). This led to research and calculations relating a dam break wave flow to tsunami surges and bores (Chanson 2005). Valentin et al. (2005) also experimented on the same concept where currents similar to those at the front of a dam break wave were expected to occur with an almost vertical bore front. Other researchers include Imai and Matsutomi (2005) and Wang et al. (1998) who also describe tsunamis to first break within offshore areas of shallow water before advancing as a bore with strong flow. Thus, a bore is widely accepted in physical experiments to imitate the front of a breaking tsunami wave at the shoreline.

Tsunamis are often represented as shallow water waves as their wave lengths are usually >20 times the water depth. On the contrary, solitary wave has also been used widely to represent tsunamis. Previous researchers such as, Synolakis (1986), Gedik et al. (2005), Thusyanthan and Madabhushi (2008) and Irtem et al. (2009) used this type of wave for their tsunami studies in the laboratory. Solitary waves are developed offshore and near-shore they transform as soliton fission. This type of wave is also described as a non-breaking tsunami wave at near shore.

Tsunami run-up as defined by the Intergovernmental Oceanographic Commission in the Tsunami glossary (IOC 2008) is the difference between the elevation of maximum tsunami penetration (inundation line) and the sea level at the time of the tsunami. Studies on tsunami run-up had been conducted by previous researchers by using physical experiments or numerical modeling. Synolakis (1986) studied run-up of long waves and presented detailed theories of the run-up distribution of non-breaking and breaking solitary waves. A schematization of a typical run-up in his studies is shown in Fig. 1. Li (2000) also did a thorough experiment on tsunami run-up regarding breaking and non-breaking solitary wave by energy conservation consideration. Simple empirical estimates of maximum run-up were produced for a breaking solitary wave condition using results from the numerical

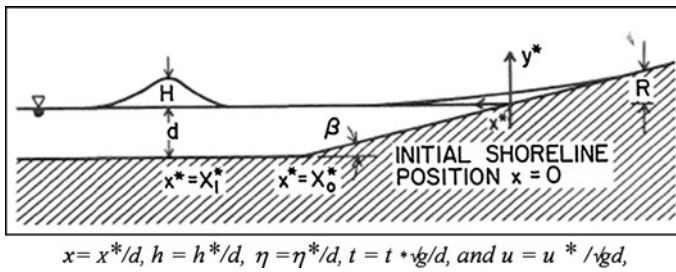


Fig. 1 Run-up schematization (Synolakis 1986)

model and validated by experimental results. The breaking type observed by Li (2000) was a plunging breaking type.

However, visual observations suggested that the run-up is a turbulent process characterized by significant scouring and sediment transport and could be related to tsunami bores. In this respect, Yeh (1991), Chanson (2005) and Sorensen (2006) used the method of advancing bore in producing the tsunami run-up in the laboratory. The transition process that took place was described and concluded to be more of a “momentum exchange” between the incident bore and the small wedge-shaped water that was initially still ahead of the bore along the shore.

2.2 Generating tsunami waves in a laboratory

There are several methods to generate tsunami waves in the laboratory. However, there are some difficulties in scaling the tsunami wave, depending on facilities available such as the length of the flume, and the objectives of the study. According to Li (2000), if the run-up process and maximum run-up are of the only parameters of interest in a study, the wave and the water flow produced after breaking can be simplified as a propagating bore, which is analogous to a shock wave in gas dynamics. It has been found from field and laboratory studies that after a wave breaks, the form of the propagating wave is similar to a propagating bore in terms of appearance.

Chanson et al. (2003) conducted an experiment creating a tsunami bore using a downstream of a plunging jet impact. The method to create a tsunami wave bore was similar to a dam break flow. It was conducted in a 15-m-long, 0.8-m-wide and 0.65-m-deep channel. The surge wave was generated by the vertical release of a known water volume through a rectangular, sharp-crested orifice (70 mm by 750 mm) at one end of the channel while a certain depth of water was already filled inside the flume. A 0.5-m high sloping beach (1V:6H) was installed at the other end. The surging flow in the channel was studied using 2 video cameras and a capacitance wave gauge for measuring the water level.

Besides Chanson et al. (2003), another method to create this type of wave is by using a gate to release instantaneously a certain amount of impounded water behind the gate. The method has been used by Yeh (1991), Ramsden (1993), Arnason (2005) and Imai and Matsutomi (2005). Ramsden (1993) stated that this method produced large bores and high-speed surges relative to what could be obtained using broken waves. Thus, using the gate allowed experiments to be conducted on a larger scale that decreases scale effects. Both Ramsden (1993) and Arnason (2005) used a pneumatic piston powered by an air compressor to lift up instantaneously a 6.4-mm-thick stainless steel gate to release a certain depth of impounded water behind the gate.

2.3 Characteristics of mangrove forest

Mangroves are trees characteristically found in tidal swamps. Figure 2 shows a schematization of a mangrove forest where *Avicennia* are found at the most seaward followed by *Rhizophora*. The mangrove forest models used in the present experiments were generally designed and constructed with reference to these species. The type of mangrove forest for this experiment is known as fringe forest where this landform comprises swamps along the shoreline that face the open sea and are directly exposed to the action of both tidal water and sea waves. Fringe forest is normally found in the tropics such as in Indonesia, Thailand and Malaysia and is being planned to be used as a defense against tsunami.

Mangrove forest is a complex combination of trunks, prop roots, pneumatophores, branches and leaves. Physically it can simply be described to consist of three parts that are the canopies, trunks and prop roots. A coastal forest provides a permeable barrier. Spacing of trees (horizontal density) and the vertical configuration of above-ground roots, stem, branches and leaves (vertical density) define the overall density (also called vegetation thickness) or the permeability of a barrier. But, in this study, only the horizontal density of the forest was considered while the vertical densities were fixed. The vertical density consists of two porosities that are the canopies, aerial roots and the trunks, while the horizontal density was recognized as the number of trees per 100 square meter.

2.4 Tidal levels

The site condition for mangroves to survive is where the ground lies between the mean sea level and the mean high water level. The typical water level during low water (LW) and high water (HW) is as shown in Fig. 3.

The vertical configuration of the mangrove restricts water flow due to drag forces and viscous forces and is expected to dissipate more tsunami wave energy. Both the forces depend on the tidal level because of the vertical profile of mangroves. The zonation and the

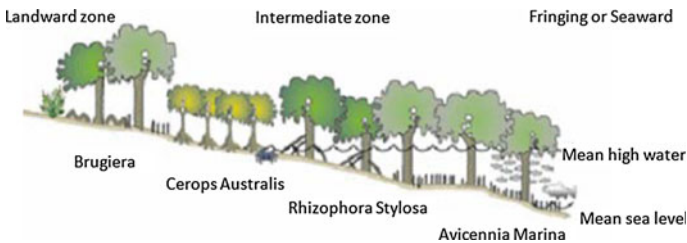


Fig. 2 Hypothetical schematization of a mangrove forest (Burger 2005)

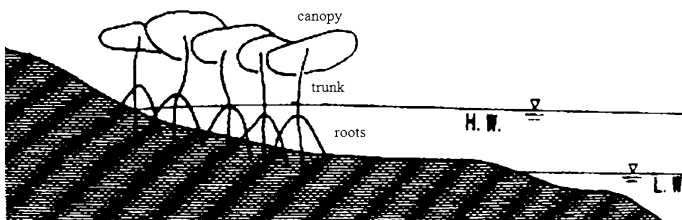


Fig. 3 Fringe forest (Cintron and Novelli 1984)

tidal level of the mangroves are also shown in Figs. 2 and 3. The energy of a tsunami could also be greatly reduced because of the substantial resistance provided by the underground roots. With low water depths, the aerial roots system causes the largest part of the wave attenuation. According to Burger (2005), mangrove canopies start to grow from around the high water level upwards. Hence, at higher water depths, trunks and canopies play a more significant role.

3 Methodology

3.1 Experimental set-up

Abd Wahab et al. (2011) conducted laboratory experiments conducted in a flume of approximately 16.6 m long, 0.92 m wide and 0.7 m high at the laboratory of Coastal and Offshore Engineering Institute (COEI), Universiti Teknologi Malaysia International Campus, Kuala Lumpur. In order to develop a tsunami in the laboratory, a very long flume is required. This is because a tsunami is known to have a very long wave length (e.g., up to 100 km at offshore). However due to space limitations, a dam break system was constructed to develop a near shore tsunami wave. Measuring marks with a minimum spacing of 0.1 m and rulers with 0.02 m spacing were drawn and installed on the slope to measure the inundation distance. The inundation distances measured are used to calculate the run-ups. Two video cameras were installed over and beside the flume for the wave and run-up observations. Four points of wave probes (P1, P2, P3, P4) were positioned along the flume to record the water levels of the tsunami flow during the experimental runs. They were located at 1, 2, 5 and 8 m from the gate. Two probes were positioned in front of the forest model and two behind it. The probes were assigned and recognized by a data acquisition software, *Geni Daq*, as C0, C2, C4 and C11 (at P4, P3, P2 and P1, respectively). The probes were calibrated before each experimental run. The uncertainty error for the calibration was ± 0.1 cm.

Figure 4a and b illustrates the set-up of the experimental work. The set-up includes the wave flume, the gate mechanism, artificial impermeable slope, wave probes and video cameras. The apparatus that were used to measure the experimental parameters are as listed in Table 1.

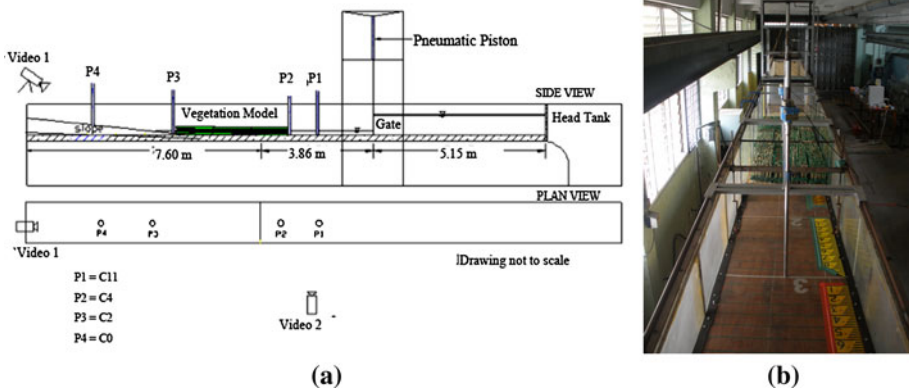


Fig. 4 Illustration (a) and image (b) of the experimental set-up

Table 1 Equipment details

No.	Equipment	Quantity	Software	Parameters measured
1	Wave probes (Endress Houser F12)	4	Geni Daq	Water surface elevation, bore/wave heights, bore/wave speed
2	Sony video camera and measuring marks installed on slope	2	Windows media player	Inundation distance, run-up
3	Gate mechanism:			
	(a) Aluminum alloy gate-grade 5083TBI (0.9 × 0.7 × 0.001 m)	1	–	–
	(b) Pneumatic actuator –HCA-FA-80B-700	1		
	(c) Compressor –Swan model: LR-115	1		

3.2 Calculation of scale factor

The mangrove height, water depth, observed tsunami height and speed were independent variables for the geometrical similarity between model and prototype. The observed mangrove heights in Malaysia and other tropical countries are between 12 and 20 m high while the tsunami heights were recorded to be between 5 and 15 m with a speed of between 12 and 14 m/s when it runs up the shore. Due to the size limitation of the wave flume which has a maximum depth of 0.2 m and in order to give space for the bore height, the coastal slope behind the mangroves model and also consideration for instant rising of the water when the bore hits the vegetation, a scale factor of 1/100 is thus adopted. Hence, for geometrical similarity, the selected average mangrove height and minimum water depth for the undistorted model are chosen to be 0.20 and 0.05 m, respectively.

For dynamic similarity and assuming a minimum prototype velocity of tsunami bores being 12 m/s, Froude similitude resulted in a velocity ratio, V_r of 1/10, thus the corresponding minimum velocity for the model was calculated to be 1.2 m/s. In order to calculate the scale factor for the bed slope, Manning equation was then used to obtain a dynamic similarity between the model and the prototype. The slope obtained here represents the beach slope that is on the landward side of the mangrove where the run-up takes place. A summary of the scaled parameters used in the experiment is shown in Table 2 below:

Table 2 Summary of scaled parameters

Scale factor	Prototype	Model
Geometric scale		
$L_r = 1/100$		
Vegetation height	20 m	0.2 m
Water depths	5–15 m	0.05–0.15 m
Dynamic scale		
$V_r = 1/10$		
Velocities	12–14 m/s	1.20–1.4 m/s
Slope		
$S_r = 4.64$	1/50–1/150	1/11–1/32

3.3 Mangrove forest model

Replicating the prototype mangrove forest of the *Rhizophora* type, the forest model consists of three distinct parts: the canopies, the main trunk and the prop roots. The different vertical porosity of this mangrove tree differentiates it from other types of forest vegetation, and it is expected to have a higher rate of tsunami wave energy dissipation. A suitable type of material has been selected to represent the various parts of the mangrove forest model in the laboratory.

3.3.1 Canopies and roots

The mangrove canopy is made up of leaves and branches. In the physical model, the canopies are represented by porous plastic material of 5 cm thickness. The porosity of the material is estimated to be 0.93. It is calculated using the equation presented by Mazda et al. (2007) where the porosity of the mangrove canopies as well as roots is measured using the equation $\zeta = V_e/V_t$, in which the porosity ζ , is defined as the volume of empty space (V_e) in a model divided by the total model volume (V_t), with $V_e = V_t - V_s$ and V_s is the volume of solids. Figure 5 shows the porous plastics used to model the canopies. Due to difficulties in obtaining the different porosity of the material to represent the canopies, the same porosity of 0.93 is used throughout for the canopies and roots. Harada and Imamura (2002) and Hiraishi and Harada (2003) used similar porosity as the forest canopies to characterize the roots model.

The density of the forest was differentiated by varying the number of tree trunks. The densities selected had an average of 3–5, 5–7 and 8–9 trees per 100 cm². See Fig. 6.

The width of the forest is one of the most important factors in mitigating the tsunami waves. In the experiments, the widths of the mangrove forest models are set-up as 1, 2 and 3 m. Each width was varied with different forest densities. The layout of the forest model with the trees arranged in a staggered pattern is shown in Fig. 7a while the model is depicted in Fig. 7b.

3.3.2 Trunks

In the prototype, mangrove tree trunks have been observed to measure 1 m or less in diameter. Hence in the experiments, traditional rattans with diameters of 1 cm and below



Fig. 5 Plastic porous material representing the model tree canopy

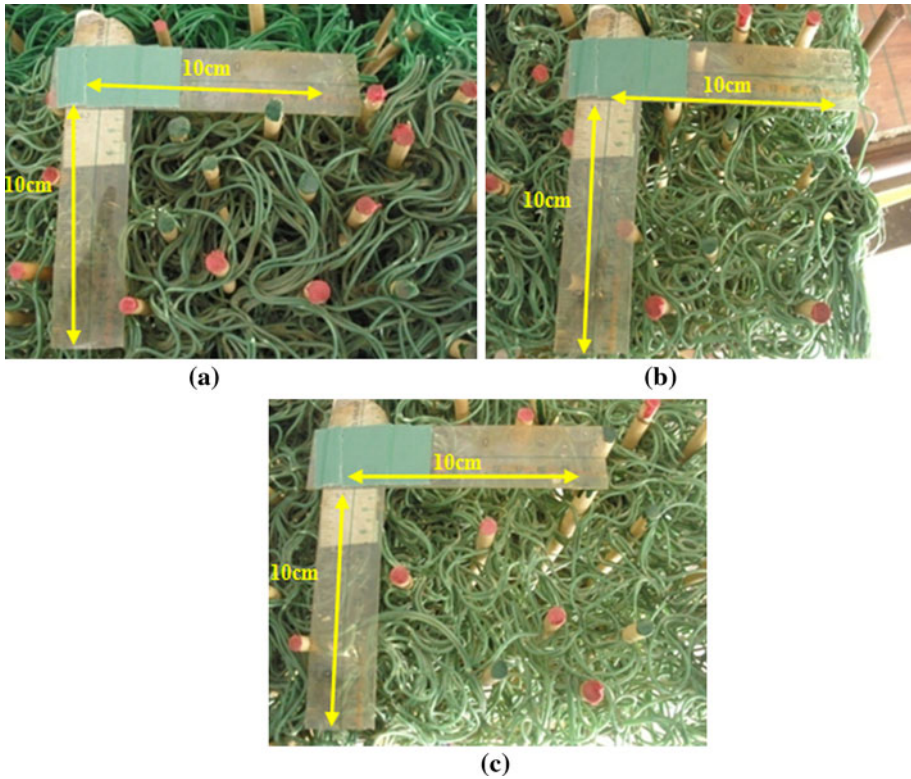


Fig. 6 a–c Density of the mangrove forest models: (a) 7–9 trees per 100 cm², (b) 5–7 trees per 100 cm², (c) 3–5 trees per 100 cm²

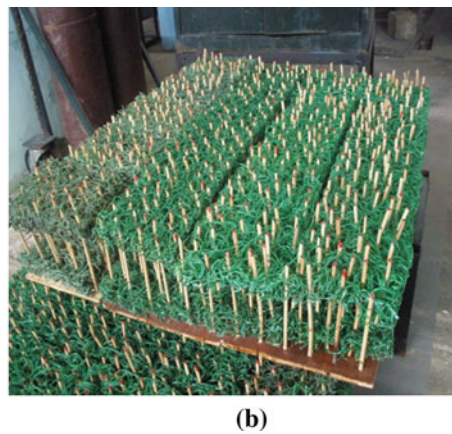
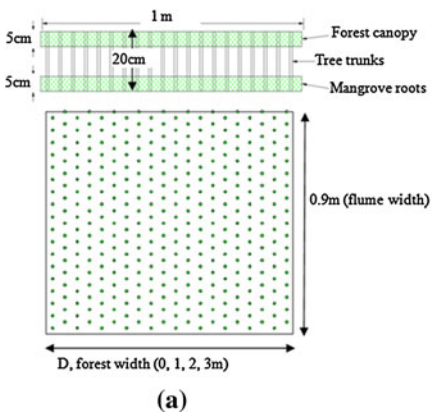


Fig. 7 Illustration of the model set-up with the (a) vegetation layout and (b) model



Fig. 8 The rattans after being cut into 20 cm lengths

were used for the trunks. Figure 8 shows the *rattans* after being cut into the required sizes (20 cm long each) for the model.

3.4 Bed slope

Adjustable slopes of 7.3 m marine plywood were installed 3.86 m from the gate to test the run-up characteristics. The slope can be adjusted to range between 1:10 and 1:50. These values are commonly used by previous researchers such as Hiraishi and Harada (2003), Harada and Imamura (2002), Yeh (1991) and Synolakis (1986). Due to limitation of the length and depth of the flume and in order to observe the relationship between run-up and slopes, only five types of slope have been considered: 1/11, 1/14, 1/17, 1/20 and 1/30. All the slopes were installed behind the vegetation which represented land slopes behind a mangrove forest. However, in this paper, only the 1/11 slope is presented and discussed.

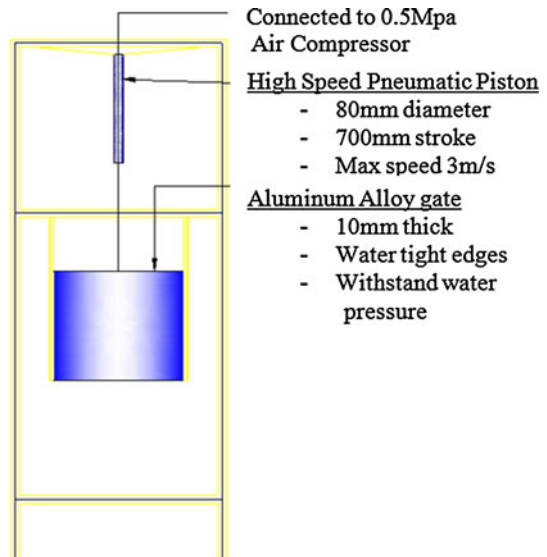
3.5 Water levels

The level of water at the instance of wave impact plays a vital role in the amount of energy dissipated due to the different resistance characteristics over the vertical profile of the mangrove tree. In this experiment, the tsunami wave characteristics were examined at two water-level conditions. First, a condition of high water (HW) was defined where the initial water level, d_3 was fixed to a level that reached just below the canopy line of the mangrove forest model which was about 0.15 m of water depth inside the flume. See Fig. 9a. The second condition was set for a low water (LW) level condition with the initial tidal level, d_3 set to be just below the level of the roots of the mangrove forest which was about 0.05 m of water level inside the flume. See Fig. 9b. The two water levels were set because mangrove



Fig. 9 Water-level settings; (a) High water and (b) Low water

Fig. 10 Gate mechanism



canopies start to grow from around the high water level upwards while at lower tide or during mean sea level, the water touches just below the mangrove roots (Burger 2005).

3.6 Modeling the tsunami waves using the dam break method

The concept of a dam break system is to instantaneously lift a gate to release a sufficient body of water impounded behind the gate to create dam break waves. These waves are associated with tsunami bores and were demonstrated by Ramsden (1993), Imai and Matsutomi (2005), Arnason (2005) and Chanson et al. (2003), Chanson (2005) who previously used the method for their tsunami physical models. The system consists of a 10-mm-thick aluminum alloy gate that was installed about 5.15 m from the end of the flume and 3.86 m from the edge of the coastal slope. The gate was powered by a pneumatic actuator with the stroke of 700 mm producing a maximum lift-off speed of 3 m/s. Figure 10 shows the concept design and mechanism of the gate.

A high-speed pneumatic piston was used for the mechanism to lift the gate instantaneously in order to create dam break waves or surge front resulting from a sudden release of a mass of fluid into the flume. The high-speed piston is powered by compressed air with

Table 3 Dam break system component specifications

Components	Specifications
Aluminum alloy gate	Grade 5083TBI (0.9 × 0.7 × 0.01 m)
High-speed pneumatic actuator	Model: HCA-FA-80B-700 Bore size: 80 mm Max stroke: 700 mm Max speed: 3 m/s Max load capacity: 250 kg
Oil-less air compressor	Model: LR-115 Max working pressure: 125 psi Capacity: 30 l Speed: 1/50 Rpm Cycle: 50 Hz

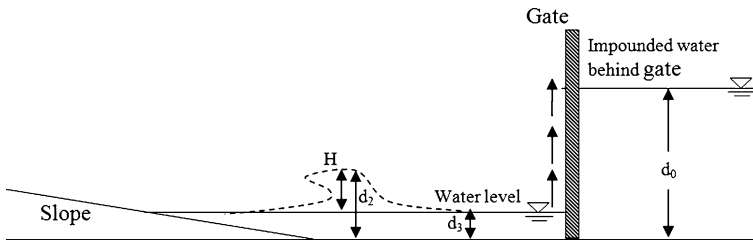


Fig. 11 Illustration of the dam break method and variables involved

a pressure of 0.5–0.8 Mpa to lift the gate with a speed of 2 ± 0.5 m/s to create the waves or bores representing the tsunami. The component specifications are shown in Table 3.

The dam break method is illustrated in Fig. 11 with H as the wave/bore height, d_2 and d_3 as the water level and tidal level, respectively, and d_0 as the impounded water level.

Desk calculations were then conducted to determine the expected waves or bores developed using the method of characteristics on the Saint–Venant equations. Properties that were considered and mainly affected the experiment are the inundation level behind the gate (upstream), d_0 , and the water level in front of the gate, d_3 . A representation of the properties can be graphically referred in Fig. 12. The results of the calculation are presented in Table 4.

Table 4 shows the expected bores or wave properties with U being the bore speed (advancing positive surge), V_2 the bore current or flow speed and $H (=d_2-d_3)$ the bore/wave height.

3.7 Experimental runs

The main objective of this study was to find the relationship between the tsunami run-up against various vegetation and tsunami wave properties, and thus, the variables involved are the run-up R , wave/bore height H , vegetation densities D and widths B , initial water level d , speed U and bed slope S . The variables involved in the experiment are shown in Fig. 13.

The experiments were run to test for three case scenarios:

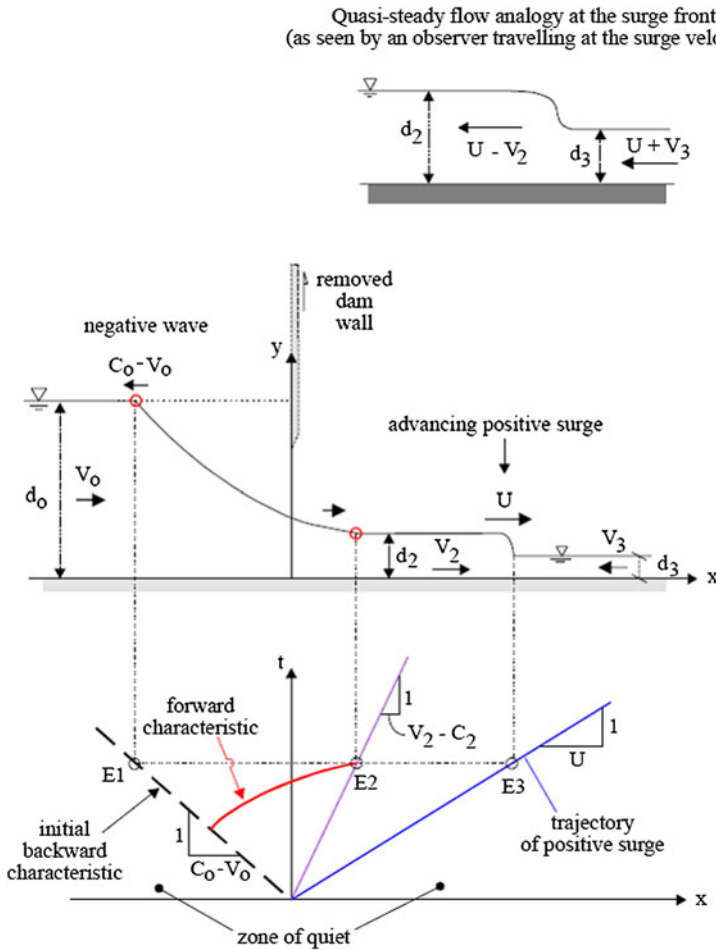


Fig. 12 Sketch of a dam break wave in a horizontal channel initially filled with water (Chanson 2005)

- Case I: Baseline scenario (without vegetation), i.e. case where $B = 0, D = 0$;
- Case II: Effects of vegetation width (B) for $B = 1, 2$ and 3 m;
- Case III: Effects of vegetation density (D) for $D = 3-5, 5-7$ and $7-9$ trees/100 cm^2 ;

In Case I experiments, preliminary runs were first conducted to test the effectiveness of the dam break system. The heights of the bores created are dependent of d_0 and d_3 as shown in Fig. 11. The selected initial test runs are presented in Table 5.

The collected data from the initial runs consisted of the bore heights or wave heights, H (m) for each tidal level and the corresponding bore or wave speed, U (m/s). The run-up and inundation length developed from the wave/bore were recorded to determine the limitation depth of the impounded water, d_0 . The limit for d_0 is when the run-up overflowed and exceeded the slope length.

After the initial test runs were conducted, the main runs for Case II and III as described in Table 6 were carried out. Results of the properties of the wave/bore developed using setup levels of d_0 and d_3 in the initial test runs were used for the main experiment runs. The experiments were conducted first by fixing the slope to 1/11 and the vegetation density to

Table 4 Calculated wave/bore properties

Water level	d_3	d_0	d_2	U	V_2	H	Water level	d_3	d_0	d_2	U	V_2	H
Low	0.05	0.10	0.07	0.93	0.32	0.02	High	0.15	0.20	0.17	1.35	0.20	0.02
	0.05	0.15	0.09	1.14	0.58	0.04		0.15	0.25	0.19	1.47	0.40	0.04
	0.05	0.20	0.10	1.32	0.82	0.05		0.15	0.30	0.21	1.58	0.59	0.06
	0.05	0.25	0.11	1.49	1.03	0.06		0.15	0.35	0.23	1.74	0.71	0.08
	0.05	0.30	0.12	1.64	1.24	0.07		0.15	0.40	0.24	1.85	0.87	0.09
	0.05	0.35	0.13	1.79	1.43	0.08		0.15	0.45	0.26	1.97	1.01	0.11
	0.05	0.40	0.14	1.93	1.61	0.09		0.15	0.50	0.27	2.08	1.15	0.12
	0.05	0.45	0.15	2.12	1.84	0.10		0.15	0.55	0.29	2.18	1.29	0.14
	0.05	0.50	0.16	2.19	1.94	0.11		0.15	0.60	0.30	2.28	1.42	0.15
	0.05	0.55	0.17	2.32	2.10	0.12		0.15	0.65	0.31	2.38	1.55	0.16
	0.05	0.60	0.17	2.44	2.25	0.12							
0.05	0.65	0.18	2.57	2.39	0.13								

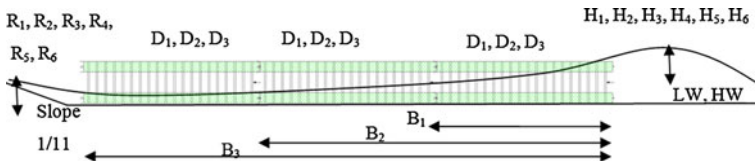


Fig. 13 Illustration of the variables involved

Table 5 Selected initial test runs

Slope	Water level, d_3 (m)		Impounded water (d_0) (m)	Collected data		Observations
	High	Low		Bore height, H (m)	Bore speed, U (m/s)	
1:11	0.15	0.05	0.20, 0.25, 0.3, 0.35, 0.4,	$H_1, H_2, H_3, H_4,$	$U_1, U_2, U_3, U_4,$	Run-up (R) and inundation distance (X_{ID})
1:14	0.15	0.05	0.45, 0.5, 0.55	H_5, H_6	U_5, U_6	
1:17	0.15	0.05				
1:20	0.15	0.05				
1:30	0.15	0.05				

D_1 (7–9 trees per 100 cm^2). The vegetation width was then varied to B_1, B_2 and B_3 (1, 2, 3 m) for each case of wave heights ($H_1, H_2, H_3, H_4, H_5, H_6$) and tidal level (HW and LW) after which the experiments were repeated with different vegetation density of D_2 and D_3 (5–7 and 3–5 trees per 100 cm^2). Run-ups ($R_1, R_2, R_3, R_4, R_5, R_6$) and their corresponding inundation lengths, X_{ID} , were observed and recorded to analyze the performance of the mangrove forest at various widths and densities.

3.8 Experimental range

The range of the parameters involved in the experiment for both model and prototype using a length scale ratio of 1:100 is presented in Table 7.

Table 6 Layout of experimental runs

Forest geometries		Hydraulic parameters Bore heights H (cm)	Water level	Data recorded
Width B (m)	Density, D (trees/100 cm ²)			
Bed slope 1:11				
0	0	H_1 H_2		(1) Water-level profiles
1	3–5	H_3	Low (LW)	(2) Bore speed, U
2	5–7	H_4	High (HW)	(3) Run-up, R
3	7–9	H_5		(4) Inundation distance, X_{ID}
		H_6		
Total number of runs = 384				

Table 7 Experimental parameter range used in (a) model and (b) prototype

Variables	H (m)	B (m)	D (trees/100 cm ²)	H/d	B/d	Dd^2
(a) Model						
HW = 0.15 m	0.025–0.14	0–3	0–8	0.17–0.93	0–20	0–18
LW = 0.05 m	0.065–0.14	0–3	0–8	1.30–2.80	0–60	0–2
(b) Prototype						
HW = 15 m	2.5–14	0–300	0–8	0.17–0.93	0–20	0–18
LW = 5 m	6.5–14	0–300	0–8	1.30–2.80	0–60	0–2

4 Results and discussion

4.1 Baseline case (without vegetation)

Initial runs were first conducted to establish the base case. These included the dam break experiments that were aimed to generate time series profiles of the waves and to investigate the run-up levels and wave speeds for the case of “no-vegetation” at the two tidal levels. Results of the experiments are described as follows:

4.1.1 Dam break experimental results

Time series profiles of the water surface just after the waves reach point P1 recorded during both high water and low water conditions are shown in Fig. 14a–b. Wave heights were measured based on the water-level profiles before the reflection time, that is $t_r = 8$ s for high water condition while $t_r = 5$ s for low water.

During the dam break experiments, observations were made on the effect of the differences between the water level behind, d_0 and in front of the gate, d_3 . With different set

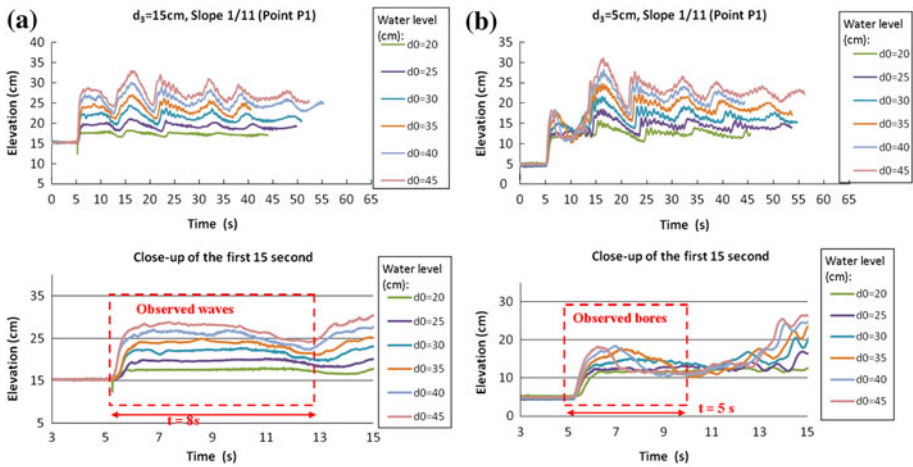


Fig. 14 Time series of the waves produced from the dam break for different cases of d_0 during (a) high water and (b) low water on slope 1/11

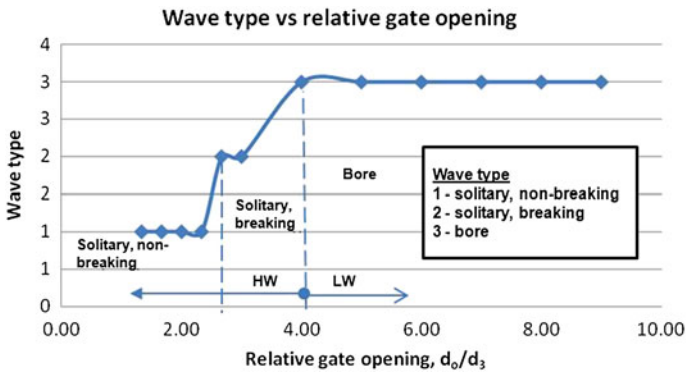


Fig. 15 Type of wave developed with respect to different water-level settings

ups of d_0 and d_3 , the experiments showed that there were two types of flow formed at different stages of the tide. When $d_0/d_3 \geq 4$ (i.e., during low water), a turbulent flow representing a tsunami bore was developed. However, for $d_0/d_3 \leq 3$ (during high water), the flow produced would represent solitary waves. On several occasions (when $2.67 \leq d_0/d_3 \leq 3$), the solitary wave could break before reaching the vegetation area. Figure 15 and Table 8 describe the type of waves developed for each case of d_0 and d_3 settings while Fig. 16 illustrates examples of images taken for the different wave types developed in the experiments. A range of 2.4–14 cm of bores and wave heights were obtained to represent the tsunami waves.

Using the Saint–Venant equation and the method of characteristics, the predicted wave heights were calculated and compared with the experimental results. A comparison between experiment and calculated wave heights is shown in Table 9 and Fig. 17.

Table 8 Type of wave produced from the dam break method

Tidal levels	Imp. water, d_0 (cm)	d_0/d_3	Wave type
High water $d_3 = 15$ cm	20	1.33	Solitary, non-breaking
	25	1.67	Solitary, non-breaking
	30	2.00	Solitary, non-breaking
	35	2.33	Solitary, non-breaking
	40	2.67	Solitary, breaking
	45	3.00	Solitary, breaking
Low water $d_3 = 5$ cm	20	4.00	Bore
	25	5.00	Bore
	30	6.00	Bore
	35	7.00	Bore
	40	8.00	Bore
	45	9.00	Bore

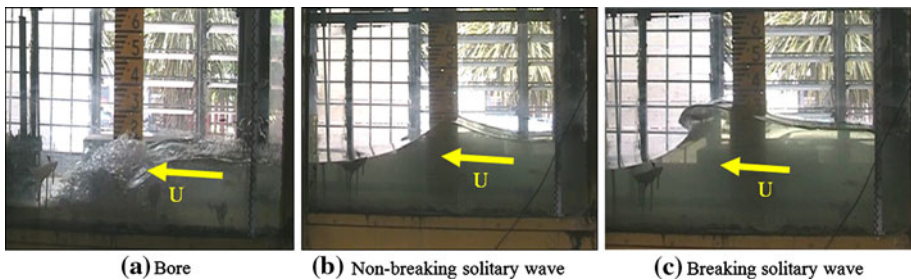


Fig. 16 a–c Types of waves produced from the dam break method

Table 9 Comparison between experimental and calculated wave/bore heights

Water level	d_3	d_0	H calc. (m)	H expt. (m)	% error
Low	0.05	0.20	0.05	0.065	29.53
	0.05	0.25	0.06	0.080	28.67
	0.05	0.30	0.07	0.100	38.14
	0.05	0.35	0.08	0.120	45.75
	0.05	0.40	0.09	0.130	42.24
	0.05	0.45	0.10	0.140	35.39
	0.15	0.20	0.02	0.025	14.01
High	0.15	0.25	0.04	0.045	11.88
	0.15	0.30	0.06	0.070	24.18
	0.15	0.35	0.08	0.095	20.27
	0.15	0.40	0.09	0.120	27.62
	0.15	0.45	0.11	0.140	27.24

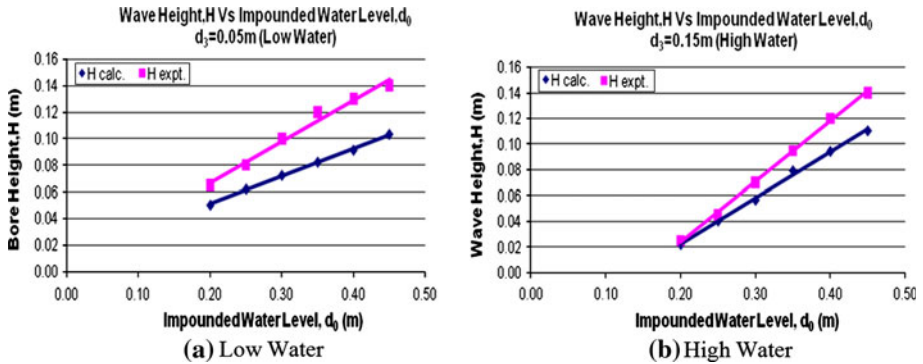


Fig. 17 a–b Comparison between experimental and calculated wave/bore heights

The percent discrepancies or error between the calculated and experimental values ranged from 11 % up to 46 %. However, wave heights during high water have lower range of errors. This could be due to the fact that the Saint–Venant equation used in the calculation of wave heights were developed for solitary waves. Even though the errors are quite large for low water, the dam break method is still relevant to be used. The errors could be due to the omission of bed friction in the calculations using the Saint–Venant equations.

4.1.2 Wave speeds

Bore/wave speed refers to the surface speed of the wave or bore as it propagates along the channel and not the flow or current speed. The experimental wave/bore speeds were measured using time period data and the distance between the probes with unit in m/s. Figure 18 presents the locations of the speed measured.

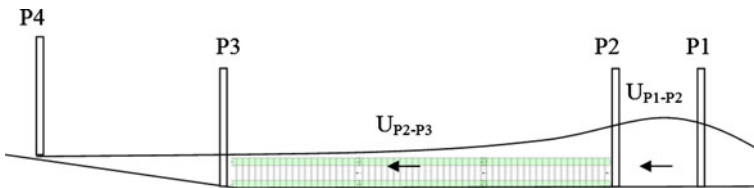


Fig. 18 Wave probe and wave/bore speed point locations

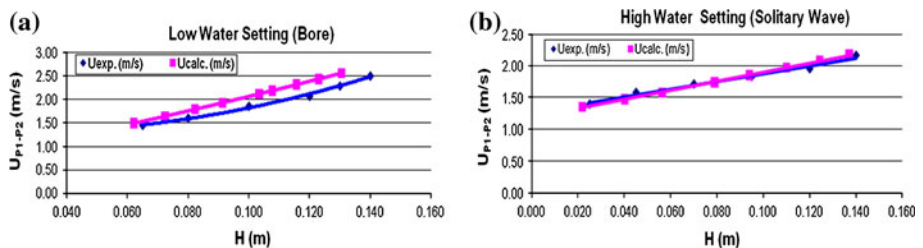


Fig. 19 a–b Bore/wave speed, U_{P1-P2} of flow before reaching the vegetation

Fig. 20 Wave/bore celerity comparison

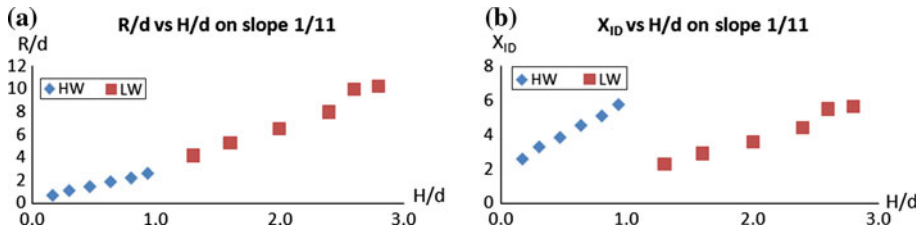
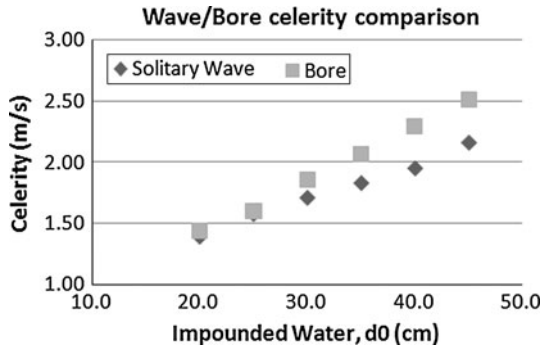


Fig. 21 Relationship between (a) relative run-up (R/d) versus relative wave height (H/d) and (b) inundation distance, X_{ID} , versus H/d on slope 1/11

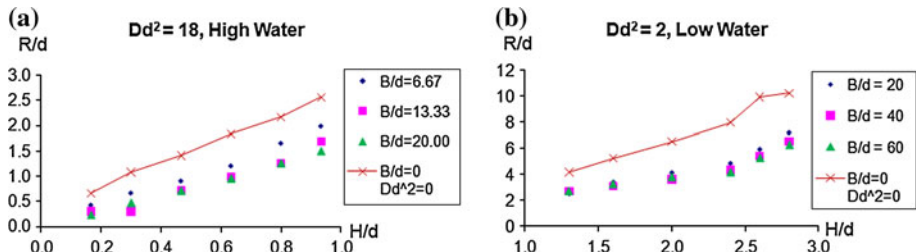


Fig. 22 Influence of vegetation width on run-up during (a) high water and (b) low water conditions

Comparisons between the measured speeds (U_{P1-P2}) with calculated speeds at the two water-level settings are shown in Fig. 19a–b. Using the scale $V_r = 0.1$, the results are consistent with calculation using the simplified methods of Saint–Venant equations and method of characteristics by Chanson (2005). It was also found that for similar settings of d_0 levels, bores have higher celerities compared to solitary waves, as shown in Fig. 20.

4.1.3 Run-up and inundation distance on non-vegetated slope

Figure 21a–b shows the plots between relative run-up R/d , and inundation distance, X_{ID} , on a slope 1/11 during low and high water, respectively. Both figures showed that both run-up and inundation distance increase correspondingly as the wave heights increase. It is also observed that larger run-ups occur when the tsunami waves approach the slope during low water.

Table 10 Percentage run-up reduction for various vegetation widths

Vegetation properties		High water			Low water		
<i>B</i> (m)	<i>D</i> (trees/100 cm ²)	<i>B/d</i>	<i>Dd</i> ²	% $\Delta R/d$	<i>B/d</i>	<i>Dd</i> ²	% $\Delta R/d$
1	4	6.7	9	23.3	20	1.0	31.0
	6		14	25.0		1.5	31.2
	8		18	32.0		2.0	36.3
2	4	13.3	9	38.9	40	1.0	33.5
	6		14	42.9		1.5	38.4
	8		18	49.6		2.0	41.3
3	4	20.0	9	42.3	60	1.0	35.4
	6		14	46.6		1.5	40.8
	8		18	49.8		2.0	41.4

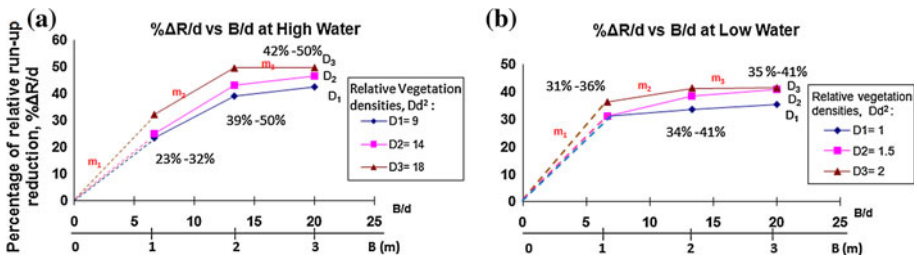


Fig. 23 Percentage of relative run-up reduction against relative vegetation width at (a) High water condition and (b) Low water condition

4.2 Case II: effects of vegetation width on run-up

The relationship between vegetation width and tsunami run-up at a particular relative vegetation density, Dd^2 , is presented in Fig. 22 in which the variations of relative run-up, R/d , with relative wave heights, H/d , for various relative vegetation widths, B/d , are shown in Fig. 22a and b during high water and low water conditions, respectively. The results are also plotted against the baseline case with no vegetation (at $B/d = 0, Dd^2 = 0$). The results are also summarized in Table 10.

It is observed that as wave heights increase, the run-up would also increase for both tidal conditions. A decrease in run-up values is apparently observed on the vegetated slope compared to the one with no vegetation. Consequently, the run-ups would also slightly decrease as the vegetation widths increase. In another analysis, the degree of run-up reductions could be observed in terms of percentages. Dimensionless plots of the percentage relative run-up reduction ($\% \Delta R/d$) due to increase in relative vegetation widths (B/d) for various relative densities (Dd^2) are shown in Fig. 23.

Table 10 shows that during high water and depending on the densities, the average percentage of run-up reduction ($\% \Delta R/d$) lies in the range of 23–32 % for the first 1 m forest width. The reduction values then increase to 39–50 % for a 2 m and 42–50 % for a 3 m forest width. However, during low water condition, the range of the average percentage run-up reduction has increased to 31–36 % for the first 1 m forest width.

This is followed by 34–41 % for the 2 m width, and about 35–41 % for a forest width of 3 m.

The results showed that the percentage run-up reduction for the first 1 m width of the vegetation at low water is higher than that which occurred at high water. Since the low water line is at about the same level as the mangrove roots, it can be inferred that mangrove roots are more effective in dissipating the wave energy compared to the trunk and its canopy. On the other hand, the steepness of slopes m_1 , m_2 and m_3 in Fig. 23 is related to the difference between the percentage reductions of the run-up between each width. For instance, Fig. 23a shows that slope m_1 is steeper than slope m_2 , followed by m_3 for all cases of vegetation densities. This implies that the percentage reduction of the run-up is higher for the first 1 and 2 m of vegetation width but not much run-up is additionally reduced as the width is increased from 2 to 3 m. Subsequently, a slightly similar reduction pattern may be observed for the low water condition as shown in Fig. 23b. Here, the degree of steepness in m_2 and m_3 is much smaller than m_1 . This again indicates that during low water, the first 1 m width of the mangrove roots is most effective in dissipating the tsunami run-up. However, the next additional 1 and 2 m width of the vegetation would not significantly improve its performance.

4.3 Case III: influence of vegetation densities on run-up

The influence of various vegetation densities on run-up at a constant forest width is shown in Fig. 24. Variations of relative run-up, R/d , with relative wave heights, H/d , for various forest densities, D , at high water are shown in Fig. 24a. Subsequently, the results at low water are presented in Fig. 24b. The results are also plotted against the baseline case with no vegetation (at $B/d = 0$, $Dd^2 = 0$). The figure shows that for all cases of forest densities, the run-up increases with increase in wave height. A decrease in run-up values is is

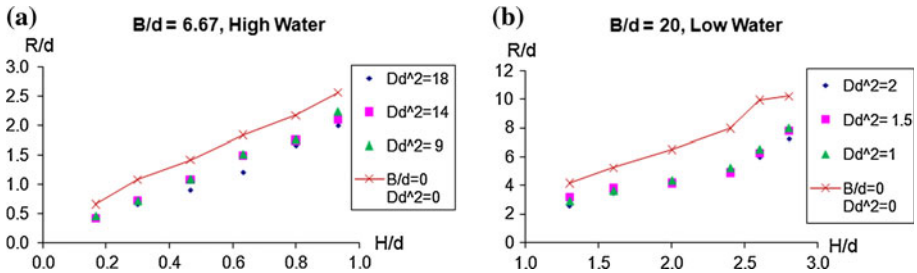


Fig. 24 Influence of vegetation densities on run-up at (a) high water condition and (b) low water condition

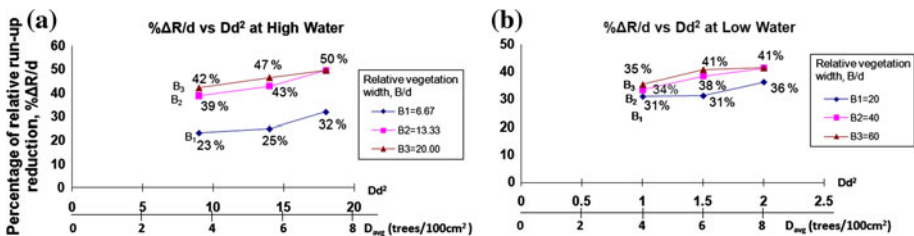


Fig. 25 Percentage of relative run-up reduction against relative vegetation Densities at (a) High water and (b) Low water

Table 11 Percentage run-up reduction for various vegetation densities

Vegetation properties		High water			Low water		
D (trees/100 cm ²)	B (m)	Dd^2	B/d	$\% \Delta R/d$	Dd^2	B/d	$\% \Delta R/d$
3–5	1	9	6.7	23.3	1.0	20	31.0
	2		13.3	38.9		40	33.5
	3		20.0	42.3		60	35.4
5–7	1	14	6.7	25.0	1.5	20	31.2
	2		13.3	42.9		40	38.4
	3		20.0	46.6		60	40.8
7–9	1	18	6.7	32.0	2.0	20	36.3
	2		13.3	49.6		40	41.3
	3		20.0	49.8		60	41.4

apparently observed on the vegetated slope compared to the one with no vegetation. Consequently, the run-ups would also slightly decrease as the vegetation densities increase. The reductions are presented in terms of percentage as shown in Fig. 25 and Table 11.

Generally, Fig. 25a shows that during high water condition, a similar relationship pattern between the run-up reductions and vegetation densities was obtained for all cases of forest width. As the vegetation density is increased, the percentage of run-up reduction would also increase. The run-ups are reduced significantly from a case without vegetation to the case with a forest density of 3–5 trees/100 cm². Not much difference is observed as the density is increased to 5–7 trees/100 cm². However, the run-up reductions are seen to be fairly increased again as the densities reach 7–9 trees/100 cm². These signify that in order for the run-up to be significantly reduced, at least another additional number of 4 trees/100 cm² would be needed.

Table 11 shows that the average percentage of run-up reduction for all cases of vegetation width falls in the range of 23–42 % for the lowest vegetation density of 3–5 trees/100 cm². For a density of 5–7 trees/100 cm², the percentage of run-up reduction was 25–47 % and 32–50 % for 7–9 trees/100 cm² during high water condition. For a low water condition, the percentage of run-up reduction lies in the range of 31–35 % for the lowest vegetation density of 3–5 trees/100 cm², and 31–41 % for density of 5–7 trees/100 cm² and 36–41 % for 7–9 trees/100 cm².

4.4 Comparison with previous studies

The experimental results were also compared with Irtem et al. (2009) who also conducted a physical model of tsunami run-up on vegetated slopes. They conducted experiments using a 1:5 slope and three cases of vegetation representing the configuration of an artificial pine tree layout. Case I represented rectilinear, Case II staggered and Case III dense rectilinear. The results were compared with the present run-up experiments that were run on slope 1/11 with representative vegetation properties of $B = 1$ m and $D = 7$ –9 trees/100 cm². The comparison is shown in the form of a graph scale as depicted in Fig. 26.

It is recognized that the method used by Irtem et al. (2009) to produce the tsunami wave was different from the present experiments; hence, different ranges of wave heights were produced. However, the data distribution still fell within the experimental range. Even though the exact width and density of the trees modeled in their experiments were not

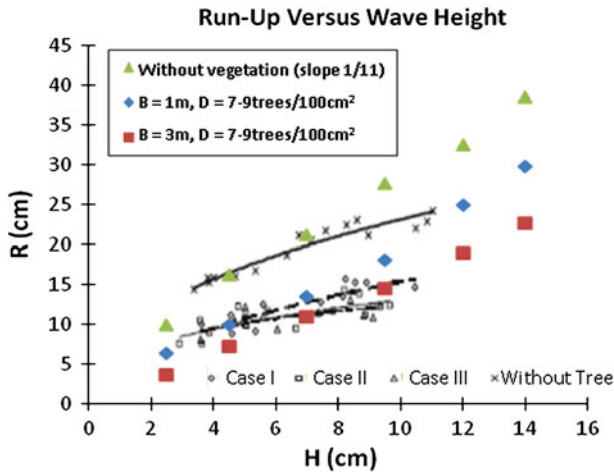


Fig. 26 Comparison of experimental results with those of Irtem et al. (2009)

described, a comparison could still be conducted by comparing the run-up distribution with several cases of modeled mangrove forest properties. A 1 m width of mangroves with a density of 8 trees/100 cm² could reduce the run-up almost similar to the artificial trees used by Irtem et al. (2009). It was also observed that for lower wave height cases, a 3 m forest width of dense mangroves would be the most effective in dissipating the tsunami energy.

5 Conclusions and recommendations

The experiments used a model to prototype scale ratio of 1:100. The dam break method used in the experiments produced two types of waves. For an initial water level of 0.05 m (representing the low water condition), a bore was developed from the instantaneous release of the impounded water level behind the gate. Subsequently, for a water level of 0.15 m representing the high water condition, a solitary wave was produced. Three types of vegetation width and density were considered for two types of tidal settings (i.e., high water and low water). A range of 1–3 m forest width and 3–5 trees/100 cm² to 7–9 trees/100 cm² of the mangrove forest model were tested to study the influence of a mangrove forest against a tsunami run-up.

The results of the experiments showed that in general, vegetation widths and densities demonstrate a dampening effect on a tsunami run-up. A larger vegetation width was found to be more effective in dissipating the wave energy. It was shown that the first 1 m width of mangrove forest could reduce 23–32 % during high water and 31–36 % during low water for a density of 3–5 trees/100 cm² to 7–8 trees/100 cm². Increasing the mangrove forest width to 2 and 3 m will further increase the average percentage of run-up reduction by 39–50 % during high water and 34–41 % during low water condition.

Vegetation densities were also found to have influence on the tsunami run-up. The denser the mangrove forest, the more run-up would be reduced. However, in this experiment, the effect of densities was found to be not as significant compared to vegetation width. For mangrove forest densities to be significant enough to reduce more tsunami run-up, an additional density of 4 trees/100 m² needs to be provided.

Water levels may also have an effect on run-up reduction. The results showed that the percentage run-up reduction for the first 1 m width of the vegetation at low water is higher than that which occurred at high water. This can also imply that mangrove roots are more effective in dissipating the wave energy compared to the trunk and its canopy since the entire height of the bore was being dissipated by the mangrove roots compared to the case during high water condition where the solitary wave was found to overtop the mangrove canopies. Hence, the ability of the vegetation to entirely dissipate the solitary wave is not encouraging. In the field, this could be interpreted that a breaking tsunami wave or tsunami bore could be effectively reduced by the first 100 m mangrove forest width when it is at low water condition. However, as the mangrove widths increase to 200 and 300 m, the degree of run-up reduction will be smaller. In fact, at the prototype scale, the first 100 m width of the mangrove forest is predicted to have the most significant effect in reducing the run-up compared to the next 200 and 300 m of the vegetation at low water. However during high water condition, a more significant reduction could be observed for a 200 m width compared to the 100 m.

It is noted that several limitations had to be considered when conducting the experiments (Alias 2010). Other than constraints in physical space, limitations such as the number of vegetation width, the diameter size of the mangrove trunks and setting the near shore coastal slope faced some technical difficulties. Additional studies including numerical modeling are thus required to further examine the influence of mangrove forest properties against the tsunami run-up in a more detailed form. Site investigation and historical data information are also important in calibrating the results. Nevertheless, the results of the physical model may prove useful for initiating design guidelines in mangrove replanting projects and in determining setback limits or buffer zones for development projects in mangrove areas.

Acknowledgments The authors wish to extend their appreciation to the Ministry of Higher Education (MOHE) Malaysia for funding the research through the Fundamental Research Grant Scheme (FRGS), vote 78122. We are also indebted to the distinguished reviewers for their constructive comments and advice.

References

- Abd Wahab AK, Ismail H, Alias NE (2011) An investigation on tsunami wave energy dissipation over vegetated coasts. Final Report Project 78122. Universiti Teknologi Malaysia
- Alias NE (2010) Tsunami run-up on vegetated coastal slopes. M.Eng Thesis, Universiti Teknologi Malaysia
- Arnason H (2005) Interactions between an incident bore and a free-standing coastal structure. University of Washington, Washington
- Burger B (2005) Wave Attenuation in mangrove forests. M.Sc. Thesis, Delft University of Technology
- Chanson H (2005) Applications of the saint-venant equations and method of characteristics to the dam break wave problem (no. CH 55/05). The University of Queensland, Brisbane, Australia
- Chanson H, Aoki S, Maruyama M (2003) An experimental study of tsunami run-up on dry and wet horizontal coastlines. *Sci Tsunami Hazards* 20(5):278–293
- Cintron G, Novelli YS (1984) Methods for studying mangrove structure. In: Snedaker SC, Snedaker JG (eds) *The mangrove ecosystem: research methods*. UNESCO, Paris, pp 91–113
- Fogarty D (2005) Tsunami-hit nations look to save mangroves. Reuters, 17 January 2005
- Gedik N, Irtem E, Kabdasli S (2005) Laboratory investigation on tsunami run-up. *Ocean Eng* 32:513–528
- Harada K, Imamura F (2002). Experimental study on the effect in reducing tsunami by the coastal permeable structures. Paper presented at the Proceedings of the Twelfth (2002) International Offshore and Polar Engineering Conference, Kitakyushu, Japan
- Harada K, Kawata Y (2005) Study on tsunami reduction effect of coastal forest due to forest growth. *Annu Disast Prevent Res Instit Kyoto Uni No.* 48C:161–165

- Hiraishi T (2000) Characteristics of Aitape tsunami in 1998 Papua New Guinea (no. 4): Report of Port and Harbour Research Institute, Japan
- Hiraishi T, Harada K (2003) Greenbelt tsunami prevention in south-pacific region (no. vol. 42, no. 2): Report of Port and Airport Research Institute
- Imai K, Matsutomi H (2005) Fluid force on vegetation due to tsunami flow on sand spit. In: Satake K (ed) *Tsunamis: case studies and recent development*. Springer, The Netherlands, pp 293–304
- IOC (2008) *Tsunami glossary*, Intergovernmental Oceanographic Commission. UNESCO IOC Technical Series, 85. Paris (English)
- Irtem E, Gedik N, Kaldasli MS, Yasa NE (2009) Coastal forest effects on tsunami run-up heights. *Ocean Eng* 36:313–320
- Kathiresan K, Rajendran N (2005) Coastal mangrove forests mitigated tsunami. *Estuar Coast Shelf Sci* 65(3):601–606
- Li Y (2000) *Tsunamis: non-breaking and breaking solitary wave run-up*. PhD Thesis, California Institute of Technology, Pasadena, California
- Mascarenhas A, Jayakumar S (2008) An environmental perspective of the post-tsunami scenario along the coast of Tamil Nadu, India: Role of sand dunes and forests. *J Environ Manag* 89(1):24–34
- Mazda Y, Wolanski E, Ridd PV (2007) *The role of physical processes in mangrove environments*. TERRAPUB, Tokyo
- Moberg F, Ronnback P (2003) Ecosystem services of the tropical seascape: interactions, substitutions and restoration. *Ocean and Coastal Management* 46. Elsevier, Amsterdam, pp 27–46
- Onrizal KC, Mansor M (2009) The effect of tsunami in 2004 on mangrove forests, Nias Island, Indonesia. *Wetl Sci* 7(2):130–134
- Ramsden JD (1993) *Tsunamis: forces on a vertical wall caused by long waves, bores, and surges on a dry bed*. Report No KH-R-54, California Institute of Technology, Pasadena, California, USA
- Sorensen RM (2006) *Basic coastal engineering* (3rd edn). New York: Springer Science+Business Media, Inc.
- Synolakis CE (1986) *The run-up of long waves*. Doctor of Philosophy Thesis, California Institute of Technology, California
- Thusyanthan NI, Madabhushi SPG (2008) Tsunami wave loading on coastal houses: a model approach. In: *Proceedings of the Institution of Civil Engineers—Civil Engineering* 161(2):77–86
- Valentin H, Jens U, Willi, H (2005) Tsunami run-up—a hydraulic perspective. *J Hydraulic Eng* 131(9): 743–747
- Wang ZY, Larsen P, Nestmann F, Dittrich A (1998) Resistance and drag reduction of flows of clay suspension. *J Hydraul Eng* 124(1):41–49
- Yanagisawa H, Koshimura S, Goto K, Miyagi T, Imamura F, Ruangrassamee A et al (2009) The reduction effects of mangrove forest on a tsunami based on field surveys at Pakarang Cape, Thailand and numerical analysis. *Estuar Coast Shelf Sci* 81(1):27–37
- Yeh HH (1991) Tsunami bore run-up. In: *Natural Hazards* (vol 4). Kluwer Academic Publisher, Dordrecht, The Netherlands